

**Thang Duong and Ralph D. Freeman**

*J Neurophysiol* 98:187-195, 2007. First published Apr 11, 2007; doi:10.1152/jn.01364.2006

**You might find this additional information useful...**

---

This article cites 44 articles, 19 of which you can access free at:

<http://jn.physiology.org/cgi/content/full/98/1/187#BIBL>

Updated information and services including high-resolution figures, can be found at:

<http://jn.physiology.org/cgi/content/full/98/1/187>

Additional material and information about *Journal of Neurophysiology* can be found at:

<http://www.the-aps.org/publications/jn>

---

This information is current as of September 22, 2008 .

# Spatial Frequency-Specific Contrast Adaptation Originates in the Primary Visual Cortex

Thang Duong and Ralph D. Freeman

Group in Vision Science, School of Optometry, Helen Wills Neuroscience Institute, University of California, Berkeley, California

Submitted 29 December 2006; accepted in final form 9 April 2007

**Duong T, Freeman RD.** Spatial frequency-specific contrast adaptation originates in the primary visual cortex. *J Neurophysiol* 98: 187–195, 2007. First published April 11, 2007; doi:10.1152/jn.01364.2006. Adaptation to a high-contrast grating stimulus causes reduced sensitivity to subsequent presentation of a visual stimulus with similar spatial characteristics. This behavioral finding has been attributed by neurophysiological studies to processes within the visual cortex. However, some evidence indicates that contrast adaptation phenomena are also found in early visual pathways. Adaptation effects have been reported in retina and lateral geniculation nucleus (LGN). It is possible that these early pathways could be the physiological origin of the cortical adaptation effect. To study this, we recorded from single neurons in the cat's LGN. We find that contrast adaptation in the LGN, unlike that in the visual cortex, is not spatial frequency specific, i.e., adaptation effects apply to a broad range of spatial frequencies. In addition, aside from the amplitude attenuation, the shape of spatial frequency tuning curves of LGN cells is not affected by contrast adaptation. Again, these findings are unlike those found for cells in the visual cortex. Together, these results demonstrate that pattern specific contrast adaptation is a cortical process.

## INTRODUCTION

Adaptation to sensory stimulation is a common feature of the nervous system. Maintained stimulation generally results in reduced neural response to a given stimulus. In the visual system, this adaptation process has been studied for different aspects of the stimulus. Contrast adaptation is probably the most frequently studied phenomenon. The initial work was limited to psychophysical approaches. Prolonged exposure to a high-contrast grating stimulus increases the contrast detection threshold for a similar stimulus (Blakemore and Campbell 1969a,b). This change in sensitivity applies only for a narrow range of spatial frequencies centered on that used for the adaptation. The threshold changes are accompanied by perceptual effects in that there is an apparent shift in perceived spatial frequency (Blakemore et al. 1970). These contrast adaptation effects can be interpreted in the context of spatial frequency selective neurons, which become fatigued by contrast adaptation (Blakemore and Campbell 1969a,b; Blakemore and Nachmias 1971; Blakemore et al. 1970; Klein et al. 1974).

Neurophysiological studies have been carried out to try to elucidate mechanisms of contrast adaptation and to attempt to localize the site(s) at which the effects occur. Single neuron studies show that cells in the primary visual cortex adjust their operating characteristics to maximize sensitivity when adapted to fixed contrast gratings. Specifically, contrast-response functions surrounding the adaptation levels have steep slopes so

that neural sensitivity is very high for small changes in contrast (Movshon and Lennie 1979; Ohzawa et al. 1982, 1985). Contrast adaptation of neurons in striate cortex is similar to that shown psychophysically in that it is selective to spatial content of the adapting stimulus, and it seems to temporarily alter spatial frequency and orientation preference (Dragoi et al. 2000, 2001; Movshon and Lennie 1979; Saul and Cynader 1989). An initial adapting stimulus for tens of seconds temporarily moves the preferred orientation and spatial frequency preference away from that of the adapting values. In the orientation domain, this effect apparently lasts for minutes (Dragoi et al. 2000).

These neurophysiological findings suggest that adaptation is a cortical phenomenon. However, intracellular recordings show tonic hyperpolarization of both lateral geniculation nucleus (LGN) and cortical cells during contrast adaptation (Carandini and Ferster 1997; Sanchez-Vives et al. 2000a,b), and this could underlie the adaptation effect. On the other hand, this cellular mechanism does not account for the pattern selective property of contrast adaptation, which has been attributed to intracortical processes (Carandini 2000; Dragoi et al. 2000, 2001; Movshon and Lennie 1979; Muller et al. 1999). With respect to sites of contrast adaptation, functional MRI (fMRI) measurements in human subjects show clear effects in V1, V2, and V3 (Boynton and Finney 2003; Fang et al. 2005; Larsson et al. 2006). In addition, V4 seems to respond to changes rather than absolute levels of contrast (Gardner et al. 2005). Pathways earlier than V1 have also been studied in single cell neurophysiological experiments. Contrast adaptation effects have been observed in LGN, but they are weak compared with those in primary visual cortex. (Ohzawa et al. 1985; Shou et al. 1996). In addition, cortical cells exhibit interocular transfer of contrast adaptation, which suggests the visual cortex as a major site of this process (Bjorklund and Magnussen 1981; Blakemore and Campbell 1969a; Sclar et al. 1985). Although there is a small degree of binocular interaction in the LGN (Haynes et al. 2005; Xue et al. 1987), it is not clear if it is sufficient for the interocular transfer of contrast adaptation.

While the visual cortex is generally assumed to be the origin of contrast adaptation (Ohzawa et al. 1982, 1985), some reports suggest that early pathways may play a role (Sanchez-Vives et al. 2000a,b; Shou et al. 1996; Smirnakis et al. 1997; Solomon et al. 2004). In the salamander retina, ganglion cells exhibit contrast adaptation that is specific for spatial scale (Smirnakis et al. 1997). In the monkey, slow contrast adaptation is observed for magnocellular but not for parvocellular cells, and

Address for reprint requests and other correspondence: R. Freeman, Univ. of California, School of Optometry, 360 Minor Hall, Berkeley, CA 94720-2020 (E-mail: freeman@neurovision.berkeley.edu).

The costs of publication of this article were defrayed in part by the payment of page charges. The article must therefore be hereby marked "advertisement" in accordance with 18 U.S.C. Section 1734 solely to indicate this fact.

simultaneous recordings of S potentials and LGN action potentials suggest that the effect originates in retinal ganglion cells (Solomon et al. 2004). Aside from the obvious possibility of species differences, it is not clear whether contrast adaptation observed in striate cortex originates from amplification of an early visual pathway mechanism. If this is the case, intracortical processes are not necessary to account for adaptation of cortical neurons.

We conducted direct tests in LGN to determine the extent to which contrast adaptation there can account for that observed in visual cortex. First, we record from LGN neurons to determine whether contrast adaptation is pattern selective. To do this, we measure the contrast-response function after adaptation to two separate spatial frequencies: one the same as that used for adaptation and the other different by an octave or more. These two spatial frequencies straddle the peak of the response curve and are at least one half an octave away from the peak spatial frequency. For neurons with low-pass response where the peak is not well defined, the two spatial frequencies are arbitrarily picked so that they are at least an octave apart and elicit equal responses. Second, we measure LGN spatial frequency tuning curves after contrast adaptation. We find that contrast adaptation in LGN is not spatial frequency selective. Additionally, we find that the shape of spatial frequency tuning curves in LGN is attenuated, but otherwise not affected by contrast adaptation. These results show that pattern-specific contrast adaptation is primarily a cortical phenomenon.

## METHODS

### Physiological preparation

All procedures complied with the National Institutes of Health Guide for the Care and Use of Laboratory Animals. Extracellular recordings were made using epoxy-coated tungsten microelectrodes in the LGN of anesthetized and paralyzed mature cats. Cats were initially anesthetized with isoflurane (1–4%). After catheterization, a continuous infusion was given of a combination of fentanyl citrate ( $10 \mu\text{g} \cdot \text{kg}^{-1} \cdot \text{h}^{-1}$ ) and thiopental sodium ( $6 \text{mg} \cdot \text{kg}^{-1} \cdot \text{h}^{-1}$ ). Bolus injections of thiopental sodium were given as required during surgery. After a tracheal cannula was positioned, isoflurane was discontinued, and the animal was artificially ventilated with a mixture of 25%  $\text{O}_2$ -75%  $\text{N}_2\text{O}$ . Respiration rate was manually adjusted to maintain an end-tidal  $\text{CO}_2$  of 34–38 mmHg. Body temperature was maintained at 38°C with a closed-loop controlled heating pad (Love Controls). A craniotomy was performed over the LGN, and the dura was resected and covered with agar and wax to form a closed chamber. After completion of all surgical procedures, continuous injection of fentanyl citrate was discontinued, and thiopental sodium concentration was lowered gradually to a level at which the cat was stabilized for 1 h or more. The level of anesthetic used was determined individually for each cat. Once a stabilized anesthetic level was reached, the animal was immobilized with pancuronium bromide ( $0.2 \text{mg} \cdot \text{kg}^{-1} \cdot \text{h}^{-1}$ ). EEG, ECG, heart rate, temperature, end-tidal  $\text{CO}_2$ , and intratracheal pressure were monitored for the entire duration of the experiment. Electrode penetrations were made perpendicular to the cortical surface at approximately Horsley-Clarke coordinates A6L9. Electrodes were advanced until visually responsive cells with LGN response characteristics were found (typically >12 mm below the cortical surface).

### Visual stimulation

Visual patterns consisting of sinusoidal gratings or noise patterns were presented on a large CRT at a frame rate of 75 Hz. The

47.8-cm-diam CRT was positioned at an optical distance of 41.8 cm in front of the cat's eyes and was split so that one half of the display stimulated the left eye and the other half stimulated the right eye. Luminance from the CRT was calibrated for a linear range with maximum and minimum values of 90 and 0.1  $\text{cd}/\text{m}^2$ , respectively.

### Extracellular recording

Single units were isolated in real time by the shape of their spike waveforms using custom software. An initial estimate of the tuning parameters was made qualitatively by computer-controlled manipulation of drifting sinusoidal gratings. Spatiotemporal receptive fields were measured with a binary m-sequence technique (Anzai et al. 1999a,b; Reid et al. 1997). The spatial extent of visual stimulation was kept slightly larger than the receptive field size. Temporal frequency tuning curves were measured with drifting sinusoidal gratings at 50% contrast. Spatial frequency and contrast tuning curves were measured at optimal temporal frequencies, typically between 4 and 15 cycles per second, determined for each cell.

### Adaptation paradigm

For each cell, three adaptation experiments were performed. These experiments used an adaptation paradigm similar to those used in previous studies (Movshon and Lennie 1979; Ohzawa et al. 1982, 1985). The first experiment measured the effect of adaptation on the contrast tuning curve at the same spatial frequency as that used for adaptation. In this experiment, the adapting stimulus was presented at 50% contrast for 60 s, followed by a series of randomized test presentations at contrast levels between 0 and 100% for 1 s each. A top-up adaptation preceded each test stimulation to maintain desired adapting levels (Movshon and Lennie 1979) as shown in Fig. 1A. The adapted contrast tuning curve was obtained from first harmonic responses.

The second experiment determined the effect of adaptation on the contrast tuning curve measured at a different spatial frequency than that used for adaptation (Fig. 1B). The adapting and test spatial frequencies were separated from the peak by at least one half an octave. Both spatial frequencies are chosen so that they elicit approximately equal firing rates. The adapting, stimulating, and top-up parameters for this experiment are similar to those for the first.

The third experiment establishes the effect of adaptation on the spatial frequency tuning curve (Fig. 1C). For each cell, we measured a spatial frequency tuning curve at 50% contrast after adaptation to a spatial frequency one half an octave above the peak. We repeated this procedure for another spatial frequency one half an octave below the peak. We used a similar adaptation scheme as that used in the first experiment.

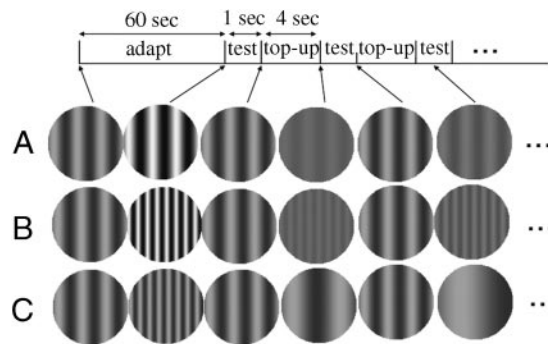


FIG. 1. Stimulation protocol for 3 adaptation experiments. Contrast response functions are measured for the same (A) or different (B) spatial frequencies as those used for adaptation. C: protocol used to measure spatial frequency tuning curve after adaptation.

## RESULTS

To examine the effects of contrast adaptation on response characteristics of LGN cells, we compared the unadapted with the adapted spatial frequency and contrast tuning curves.

The response of a typical neuron in the LGN to an adapting grating is shown in Fig. 2A. In this case and for another 40 cells, we presented a sinusoidal grating of 50% contrast drifted at optimal temporal frequency for 60 s. The poststimulus time histogram (PSTH) of Fig. 2A shows a typical exponential decay pattern indicated by the solid line. Most neurons exhibit similar exponential decay patterns in response to the onset of an adapting grating. We fit this decay with the function

$$r(t) = (A - B)e^{-t/\tau} + B \quad (1)$$

where  $r(t)$  is the spike response at time  $t$ ,  $A$  is the maximum response,  $B$  is the adapted response,  $t$  is time since stimulus onset, and  $\tau$  is the adaptation time constant. The average normalized adapted response (defined as  $B/A$ ) for our population of 38 cells was  $79.44 \pm 3.67\%$  of the unadapted level, which is consistent with an earlier report (Shou et al. 1996) in which a similar protocol was used. A histogram that shows the distribution of adapted response levels for our population of cells is presented in Fig. 2B (bottom). A similar histogram of the adaptation time constant is shown in Fig. 2B (top).

To confirm that the adaptation effects are reversible, we measured the recovery process in six cells by first testing unadapted response characteristics. We adapted each cell,

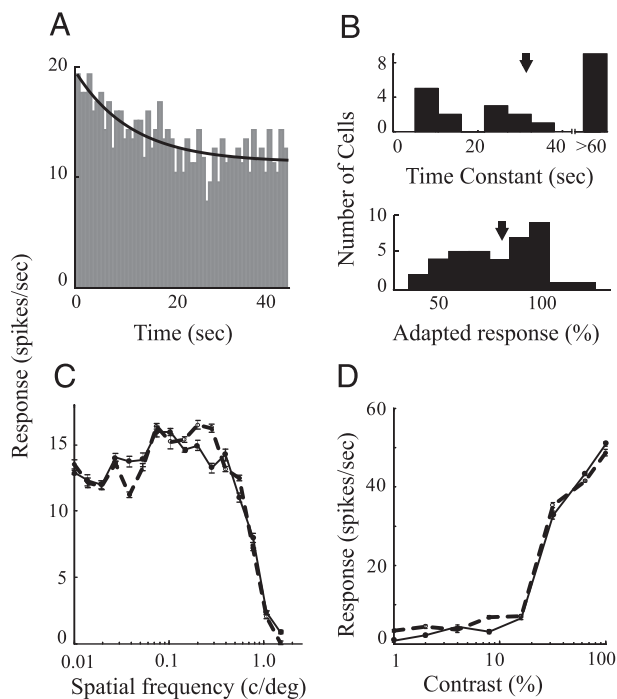


FIG. 2. A: A poststimulus time histogram (PSTH) of the response to an onset of a 50% contrast drifting grating for a representative lateral geniculate nucleus (LGN) cell. Solid line denotes best fitted exponential decay function. B: histogram of response after adaptation (bottom) normalized as a percent of response before adaptation and time constant (top) defined as time required to reach 90% of maximum adaptation level. Arrows indicate population means. C: control (dashed lines) and recovery (solid lines and filled circles) spatial frequency tuning curves. D: similar control data for contrast tuning. Both sets of data (C and D) were obtained for identical stimulation conditions separated by 10 min.

waited for  $\geq 10$  min during which the cell was not stimulated, and retested the response characteristics using the original stimulation protocol. Data for one of these control tests are shown in Fig. 2, C and D. Initial (Fig. 2, C and D, filled circles; solid lines) and recovery data (Fig. 2, C and D, empty circles; dashed lines) for spatial frequency (Fig. 2C) and contrast tuning (Fig. 2D) functions are closely matched. The other five control tests yielded similar results.

Contrast adaptation in primary visual cortex of the cat has been shown to alter contrast-response functions. The adapted contrast tuning function shifts toward the right of the unadapted measurement (Ohzawa et al. 1982, 1985). A similar response characteristic has been reported for M-cells in the monkey LGN (Solomon et al. 2004). To explore this effect directly in the cat's LGN, we determined the change in contrast-response functions before and after adaptation. Figure 3, A–D, shows contrast-response functions of four representative cells before and after adaptation. Filled circles and solid lines represent unadapted contrast-response functions. Empty circles and dotted lines represent adapted contrast-response functions. The lines represent the best hyperbolic nonlinearity fits given by the equation (Albrecht and Hamilton 1982)

$$r(c) = \frac{R_{\max}c^n}{c^n + C_{50}^n} + B \quad (2)$$

where  $r(c)$  is the response to contrast  $c$ ,  $R_{\max}$  is the maximum response of the cell,  $C_{50}$  is the contrast for which the discharge rate is half-maximum, and  $B$  and  $n$  are free parameters. In general,  $R_{\max}$  and  $C_{50}$  represent the response and contrast gain of the cell, respectively (Albrecht and Hamilton 1982). According to Eq. 2, a right or leftward shift in the contrast tuning curve corresponds, respectively, to an increase or decrease in  $C_{50}$ . For 14 of 26 cells, we found a small reduction in  $R_{\max}$  and for 21 of 26 cells, an increase in  $C_{50}$  was observed after adaptation, as shown in Fig. 3, A and B. For 12 of 26 cells, either no change or an increase was found in  $R_{\max}$ , and for 5 of 26 cells, there was no change or a small decrease in  $C_{50}$  as shown in Fig. 3, C and D. A comparison of adapted and unadapted  $R_{\max}$  and  $C_{50}$  for our population of LGN cells is shown in Fig. 4, A and B. Unadapted and adapted  $R_{\max}$  values appear equally distributed along the unity line, and there is a small decrease ( $7.7 \pm 6.9\%$ ) in the average value after adaptation (Fig. 4A; different from 0;  $P < 0.3$ ). On the other hand,  $C_{50}$  increased substantially after adaptation by an average of  $37.25 \pm 10.30\%$  (Fig. 4B; significantly different from 0;  $P < 0.001$ ). These results confirm that adaptation effects are exhibited by neurons in the LGN.

Contrast adaptation of cortical neurons is selective for spatial frequency. Therefore adaptation to a grating of a given spatial frequency has minimal effect on the contrast-response function tested at a different spatial frequency (Movshon and Lennie 1979; Muller et al. 1999). This is a central feature of contrast adaptation in visual cortex, and it is important to determine whether this applies to neurons in the LGN. We tested our population of cells using a similar paradigm as that used for visual cortex (see METHODS). Figure 5, A–D, shows the same data as in Fig. 3, A–D, with an additional adaptation condition in which the spatial frequency of the adapting grating is different, but the spatial frequency of the test stimuli remains the same. Results of this additional test (Fig. 5, A–D, empty

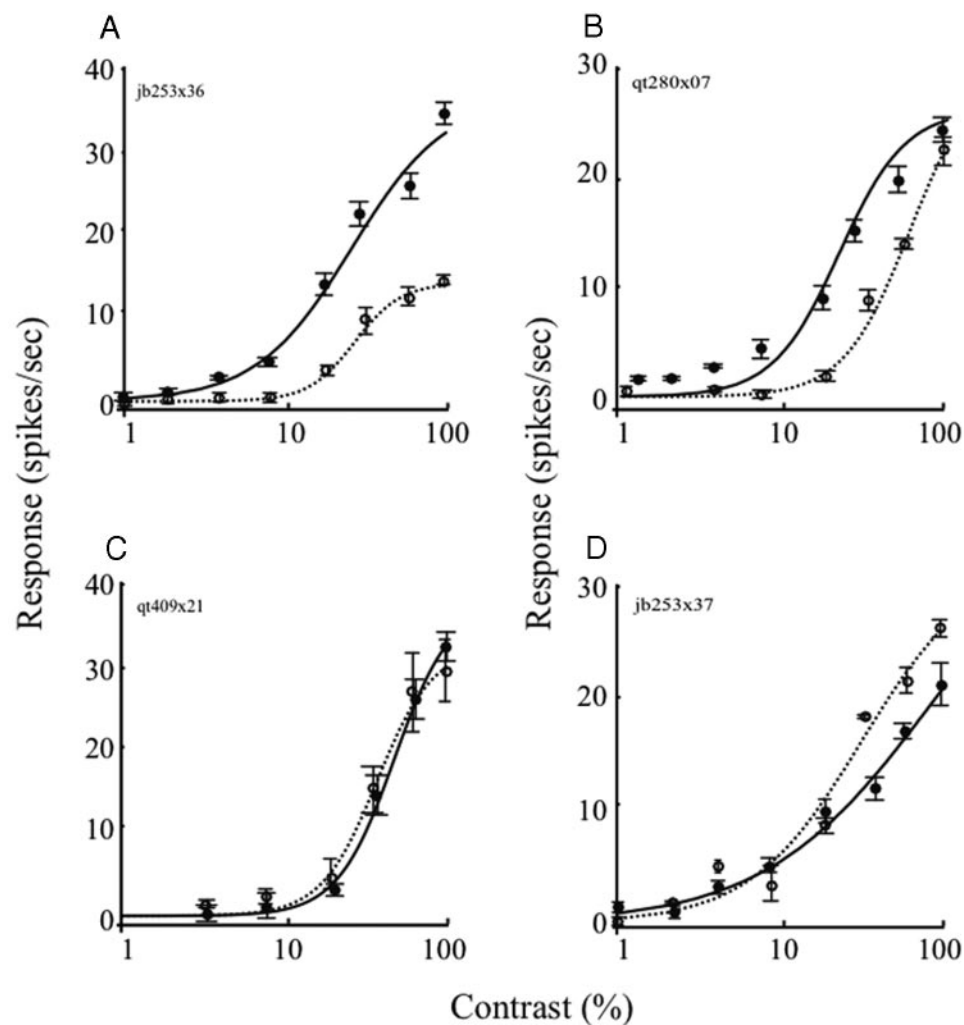


FIG. 3. Contrast response functions before and after adaptation for 4 representative LGN cells. Filled and empty circles denote responses in unadapted and adapted conditions, respectively. Solid and dotted lines are best hyperbolic nonlinearity fits to data points. Spatial and temporal frequencies for test stimuli are (A) 0.26 cpd and 14 Hz, (B) 0.5 cpd and 10 Hz, (C) 0.07 cpd and 12 Hz, and (D) 0.3 cpd and 7 Hz. Adapting grating has the same temporal and spatial frequencies as the test.

triangles and dotted lines) show clearly that the effect of contrast adaptation is independent of the adapting spatial frequency. This is shown by the finding that contrast-response functions are similar after adaptation to two widely different spatial frequencies.

For a subset of our LGN cell population ( $n = 23$ ), we determined responses for two conditions. In one, the same

spatial frequency was used for adaptation and for determining contrast-response functions. For the second condition, the test spatial frequency differed from that used for adaptation by more than an octave. Results for these two conditions are presented in Fig. 6 for  $R_{\max}$  (A) and  $C_{50}$  (B) values. The horizontal axes denote  $R_{\max}$  and  $C_{50}$  values for contrast tuning curves measured after adaptation to the same spatial frequency

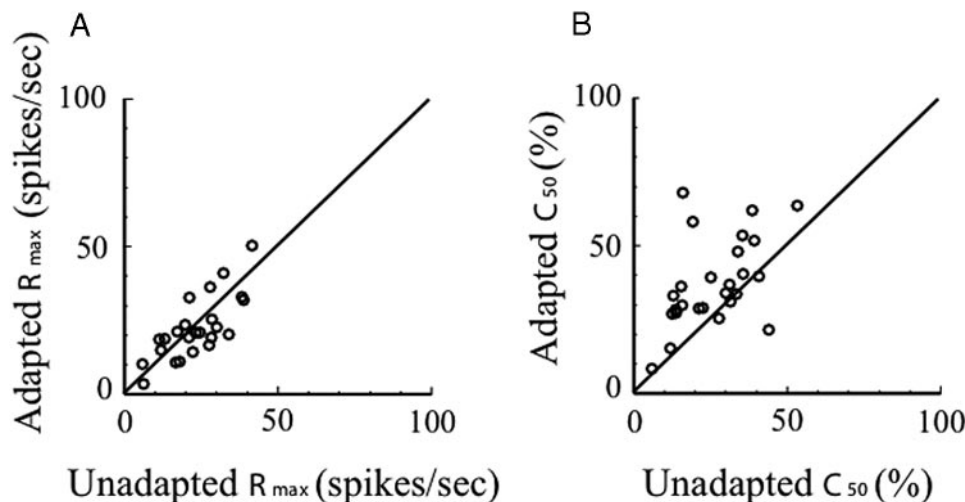


FIG. 4. Change in contrast tuning parameters caused by adaptation. A:  $R_{\max}$  for adapted vs. unadapted conditions. B:  $C_{50}$  in adapted vs. unadapted conditions.

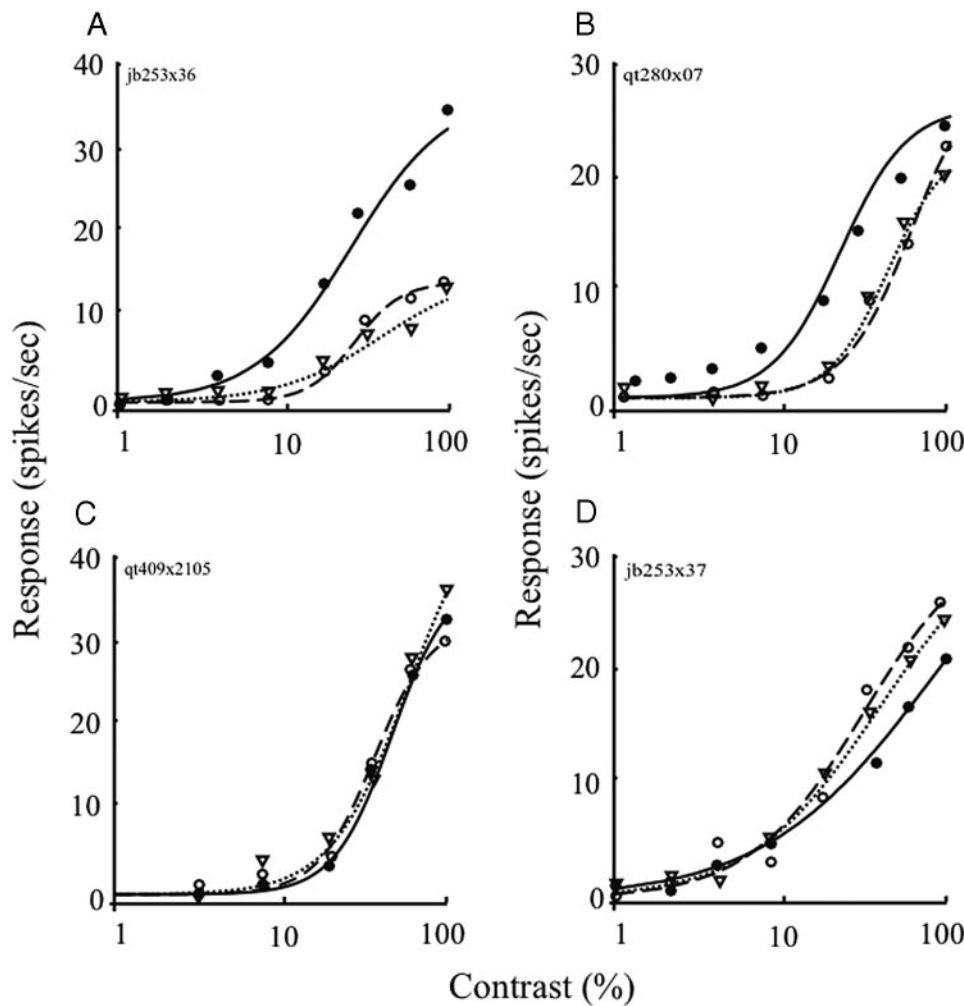


FIG. 5. Same data as in Fig. 3 with an additional adaptation condition in which adapt and test spatial frequencies are different, denoted by empty triangles and dotted lines. For these additional experiments, test spatial and temporal frequencies and adapting temporal frequencies are the same as in Fig. 3, and adaptation spatial frequencies are (A) 0.1, (B) 0.1, (C) 0.53, and (D) 0.02 cpd.

as that of the test. Vertical axes denote  $R_{max}$  and  $C_{50}$  values for contrast tuning curves measured after adaptation to a different spatial frequency than that of the test stimulus. The diagonals are unity lines. The data show that most points cluster around the unity lines for both  $R_{max}$  and  $C_{50}$ . Therefore the effects of contrast adaptation on  $R_{max}$  and  $C_{50}$  are independent of the adapting spatial frequency.

The other aspect of contrast adaptation in the visual cortex that must be addressed has to do with the observation that changes are observed in tuning properties. Temporary alterations in orientation (Dragoi et al. 2000, 2001; Muller et al. 1999) and spatial frequency tuning (Movshon and Lennie 1979; Saul and Cynader 1989) of cells in the visual cortex have been observed as a consequence of contrast adaptation. We

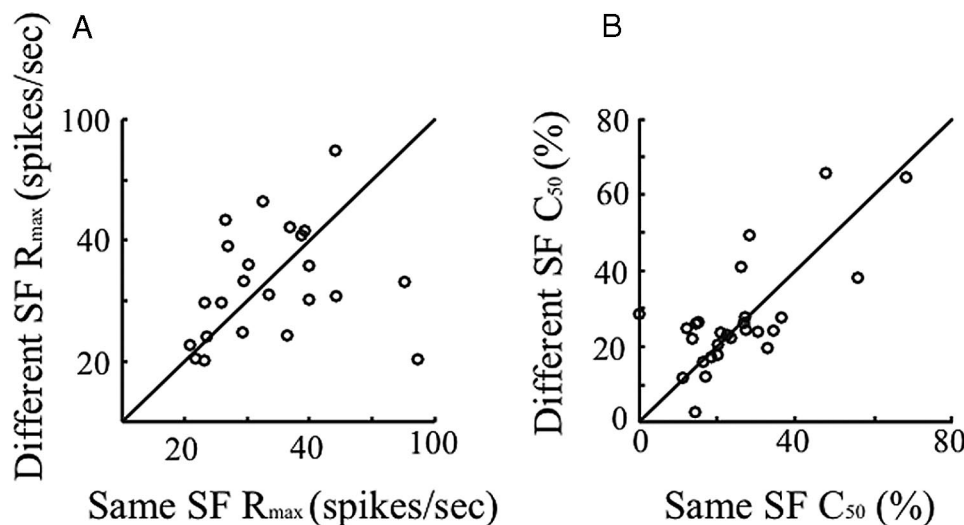


FIG. 6. Comparison of  $R_{max}$  (A) and  $C_{50}$  (B) for 2 conditions. One is adaptation to a different spatial frequency than that of the test. Second condition is adaptation to same spatial frequency as that of the test.

wanted to determine whether contrast adaptation has similar effects on spatial frequency responses in LGN. To address this question, we measured the spatial frequency tuning curves before and after adaptation to two different spatial frequencies separated by an octave or more. Figure 7, A–D, shows data from four representative LGN neurons. Unadapted (filled circles, solid lines) and two adapted spatial frequency tuning curves (empty circles, dashed lines and empty triangles, dotted lines) are included. The adapted tuning curves were measured with two different adaptation spatial frequencies that are at least one octave apart. The arrows above the plots denote the adapting spatial frequencies, which consist of one above (empty triangle, dotted line) and one below (empty circle, dashed line) the tuning peaks. For these two of the four example cells (Fig. 7, A and B) and for 14 of 19 cells, adaptation decreases the amplitude of the spatial frequency tuning curve while keeping the tuning peak and width approximately constant. The other two example cells (Fig. 7, C and D) and the remaining neurons show either an increase in amplitude or no change and relatively constant width and peak values.

To quantify the effects of adaptation on spatial frequency tuning, we fit each tuning curve with a Gaussian function

$$r(f) = Ae^{-\frac{(f-\mu)^2}{2\sigma^2}} + B \quad (3)$$

where  $r(f)$  is the response at spatial frequency  $f$ ,  $\mu$  is the mean,  $\sigma$  is the width,  $A$  is the amplitude, and  $B$  is a free offset parameter. The data shown in Fig. 8, A and B, compare the peaks and widths, respectively, of 19 LGN cells for adapted (vertical axis) and unadapted (horizontal axis) conditions. For each cell, the empty and filled circles denote adaptation to low and high spatial frequency conditions, respectively. Therefore there are two data points for each cell in Fig. 8, A and B. For most cells, the peaks and widths remain constant for unadapted and adapted conditions. In other words, adaptation does not change the peaks and widths of the spatial frequency tuning curves (Fig. 8, A and B). Linear regression analysis of adapted versus unadapted peak spatial frequencies yields  $R^2 = 0.79$ , slope = 1.04 (not significantly different from 1;  $P > 0.5$ ). Regarding tuning width, we find that it decreases after adaptation for most cells. However, a similar linear regression analysis of adapted versus unadapted spatial frequency tuning

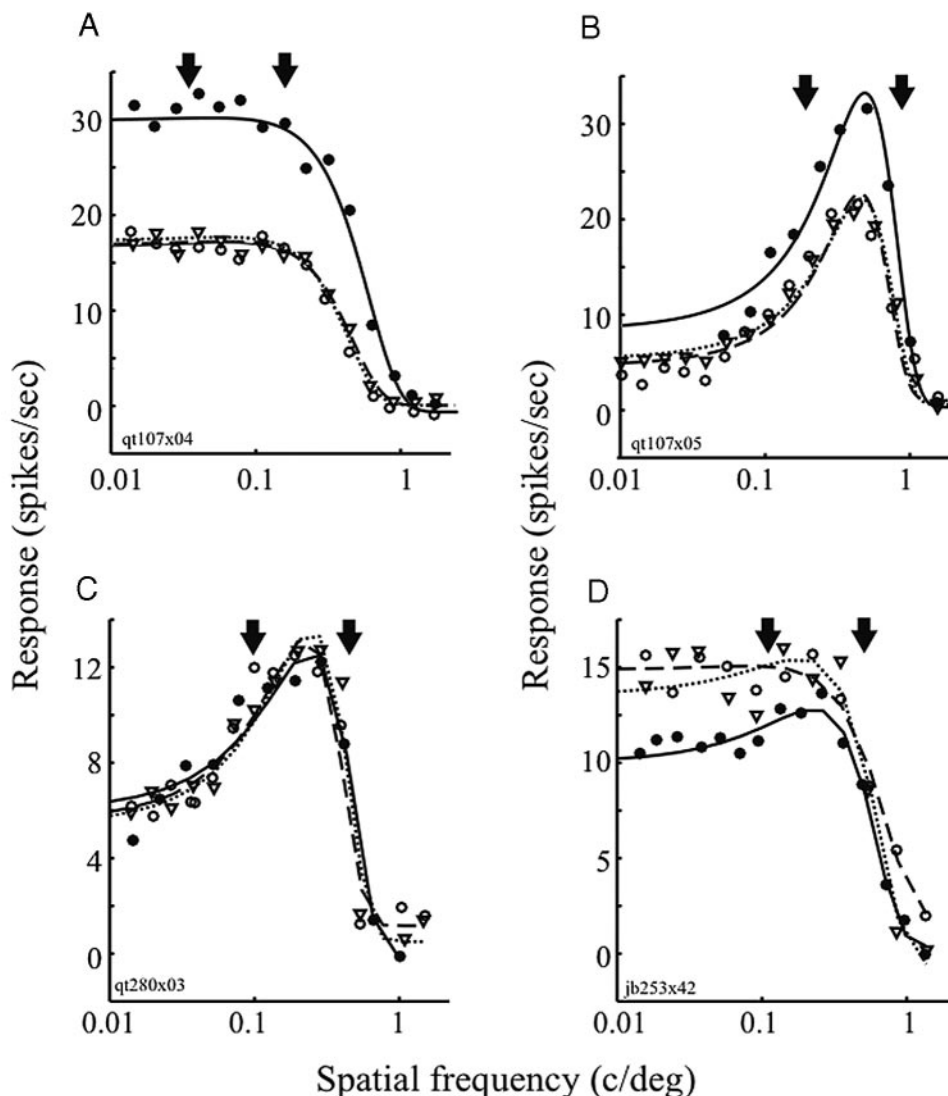


FIG. 7. Spatial frequency tuning curves for 4 representative cells before adaptation (filled circles, solid line), after adaptation to a spatial frequency below the peak (empty circles, dashed line), and after adaptation to a spatial frequency above the peak (empty triangles, dotted line). Lines denote best Gaussian function fits to data. Spatial frequency tuning curves for both conditions of adaptation are almost identical for all 4 cells. Temporal frequencies of adapting and test stimuli are (A) 10, (B) 7, (C) 7, and (D) 10 Hz.

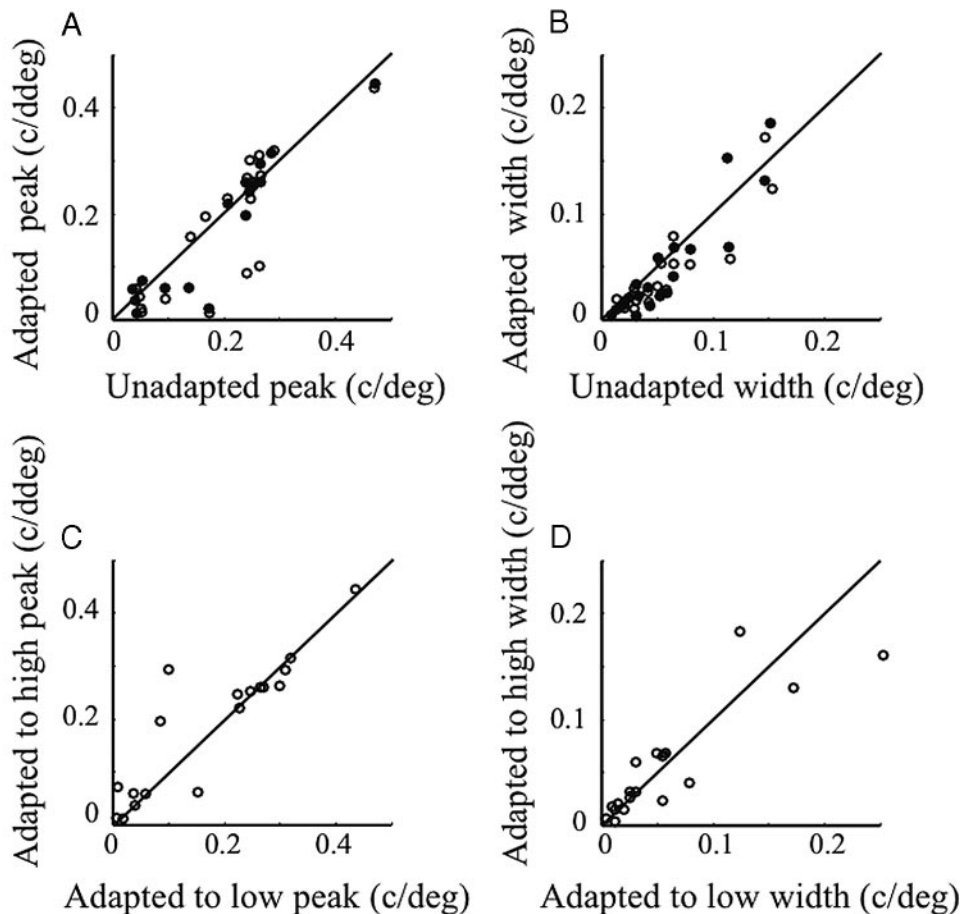


FIG. 8. Difference in spatial frequency tuning curve parameters in 3 conditions: unadapted, adapted to low spatial frequencies, and adapted to high spatial frequencies. *A*: adapted (vertical axis) vs. unadapted (horizontal axis) spatial frequency tuning peak ( $\mu$  parameter). Empty and filled circles denote adaptation to a spatial frequency below (low) and one above (high) peak, respectively ( $n = 19$ ). *B*: adapted (vertical axis) vs. unadapted (horizontal axis) spatial frequency tuning width ( $\sigma$  parameter). Empty and filled circles denote adaptation to a spatial frequency below (low) and a spatial frequency above (high) peak, respectively ( $n = 19$ ). *C*: spatial frequency tuning peaks after adaptation to a high (vertical axis) spatial frequency vs. a low (horizontal axis) one, respectively ( $n = 19$ ). *D*: spatial frequency tuning widths ( $\sigma$  parameter) after adaptation to a high (vertical axis) spatial frequency vs. a low (horizontal axis) one, respectively ( $n = 19$ ).

widths gives  $R^2 = 0.72$ , slope = 1.13 (not significantly different from 1;  $P > 0.75$ ). Therefore contrast adaptation does not significantly affect the spatial frequency tuning curves of LGN cells.

Figure 8, *C* and *D*, shows the tuning peaks and widths, respectively, for 19 cells after adaptation to spatial frequencies below (horizontal axis) and above (vertical axis) the tuning peaks. These cells clearly cluster along the unity line. Linear regression analysis of the spatial frequency tuning peak for adaptation to high versus low spatial frequencies yields  $R^2 = 0.79$ , slope = 0.86 (not significantly different from 1;  $P > 0.75$ ). Similar linear regression analysis for the width parameter gives  $R^2 = 0.82$ , slope = 0.92 (not significantly different from 1;  $P > 0.6$ ). Therefore the effect of contrast adaptation on the spatial frequency tuning curves is independent of the adapting spatial frequencies.

#### DISCUSSION

We have considered the origin of a common sensory reaction to persistent activation of a neural system. The case we have examined is the effect of a high-contrast visual stimulus that temporarily reduces and alters sensitivity to a stimulus in the visual pathway. Although previous studies of contrast adaptation have generally considered it to be based on cortical circuits, a careful examination of the literature shows that there is a clear effect at the LGN level. In particular, Ohzawa et al. (1985) (see Fig. 5) show that most cells in the LGN adapt to some extent, although not nearly to the degree of neurons in the

visual cortex. Subsequent studies using different approaches confirm this result (Sanchez-Vives et al. 2000b; Shou et al. 1996; Solomon et al. 2004). Results are not uniform, and in one, contrast adaptation is reported to be absent in LGN cells (Mante et al. 2005). However, data are shown for only one cell, so it is not clear how that conclusion was reached. In any case, there is sufficiently clear evidence of contrast adaptation in LGN to consider the possibility that the effects observed in visual cortex have their origin in early visual pathways. This could be initiated at the ganglion cell stage of the retina. To rule this out, we conducted tests which showed that adaptation effects in LGN are clearly different from those found in visual cortex. A strong indicator is that adaptation is not spatial frequency specific in LGN. We conclude that the origin of spatial frequency specific contrast adaptation and presumably other types of pattern specific visual adaptation is in the visual cortex.

Visual adaptation to high-contrast gratings has perceptual consequences in humans. First, adaptation increases the contrast detection threshold for a stimulus of a similar pattern. This only holds for a narrow range of orientations and spatial frequencies surrounding that of the adapting pattern (Blake-more and Campbell 1969b). Second, apparent subjective contrast levels are reduced after adaptation (Barrett et al. 2002; Ross and Speed 1996; Snowden and Hammett 1992, 1996). Third, discrimination thresholds may be enhanced by contrast adaptation (Abbonizio et al. 2002; Greenlee and Heitger 1988; Maattanen and Koenderink 1991). These perceptual conse-

quences have been attributed to fatigue of neuronal channels, which decreases their subsequent response strengths. This decrease in strength, in turn, has an effect on perception (Blakemore and Campbell 1969a,b; Blakemore and Nachmias 1971; Blakemore et al. 1970, 1973; Klein et al. 1974).

The neural basis of these perceptual contrast adaptation effects is thought to be located in primary visual cortex. Fatigue of neurons in cortex is mediated by a tonic hyperpolarization that accompanies contrast adaptation (Carandini and Ferster 1997; Sanchez-Vives et al. 2000a,b). However, similar hyperpolarization processes have been shown in LGN neurons (Sanchez-Vives et al. 2000a,b). In addition, S potential recordings in the LGN implicate retinal origins of adaptation effects (Solomon et al. 2004). Therefore potential mechanisms of contrast adaptation may be located in early pathways as well as in the primary visual cortex. Neural fatigue alone, however, cannot completely account for contrast adaptation of cortical neurons, because this process is specific to the adapting pattern (Carandini 2000). This pattern specificity is thought to be essential to account quantitatively for perceptual consequences of contrast adaptation in humans (Jin et al. 2005; Klein et al. 1974). Our data show that, unlike cortical neurons, LGN cells do not exhibit spatial frequency-specific adaptation. Therefore cortical mechanisms must be responsible for generating spatial frequency specific adaptation. Presumably, this also applies to pattern specific adaptation in general.

We should note that retinal ganglion cells in the salamander exhibit slow-contrast adaptation of a similar time-course and magnitude as that found for visual cortex (Smirnakis et al. 1997). Furthermore, this effect does not transfer over spatial scale. Two factors may account for the difference between this result and our findings. First, white noise at different spatial scales was used in the salamander experiments, in contrast to our drifting grating stimulation. Second, sophisticated retinal circuits have been found in lower-order animals that may not exist in cats and primates (Barlow and Levick 1965; Barlow et al. 1964; Fried et al. 2002). Therefore it is possible that the difference between our results and those on salamander retina may be species based.

#### GRANTS

This work was supported by National Eye Institute Research and Core Grants EY-01175 and EY-03176.

#### REFERENCES

- Abbonizio G, Langley K, Clifford CW.** Contrast adaptation may enhance contrast discrimination. *Spat Vis* 16: 45–58, 2002.
- Albrecht DG, Hamilton DB.** Striate cortex of monkey and cat: contrast response function. *J Neurophysiol* 48: 217–237, 1982.
- Anzai A, Ohzawa I, Freeman RD.** Neural mechanisms for processing binocular information I. Simple cells. *J Neurophysiol* 82: 891–908, 1999a.
- Anzai A, Ohzawa I, Freeman RD.** Neural mechanisms for processing binocular information II. Complex cells. *J Neurophysiol* 82: 909–924, 1999b.
- Barlow HB, Hill RM, Levick WR.** Retinal ganglion cells responding selectively to direction and speed of image motion in the rabbit. *J Physiol* 173: 377–407, 1964.
- Barlow HB, Levick WR.** The mechanism of directionally selective units in rabbit's retina. *J Physiol* 178: 477–504, 1965.
- Barrett BT, McGraw PV, Morrill P.** Perceived contrast following adaptation: the role of adapting stimulus visibility. *Spat Vis* 16: 5–19, 2002.
- Bjorklund RA, Magnussen S.** A study of interocular transfer of spatial adaptation. *Perception* 10: 511–518, 1981.
- Blakemore C, Campbell FW.** Adaptation to spatial stimuli. *J Physiol* 200: 11P–13P, 1969a.
- Blakemore C, Campbell FW.** On the existence of neurones in the human visual system selectively sensitive to the orientation and size of retinal images. *J Physiol* 203: 237–260, 1969b.
- Blakemore C, Muncey JP, Ridley RM.** Stimulus specificity in the human visual system. *Vision Res* 13: 1915–1931, 1973.
- Blakemore C, Nachmias J.** The orientation specificity of two visual after-effects. *J Physiol* 213: 157–174, 1971.
- Blakemore C, Nachmias J, Sutton P.** The perceived spatial frequency shift: evidence for frequency-selective neurones in the human brain. *J Physiol* 210: 727–750, 1970.
- Boynton GM, Finney EM.** Orientation-specific adaptation in human visual cortex. *J Neurosci* 23: 8781–8787, 2003.
- Carandini M.** Visual cortex: fatigue and adaptation. *Curr Biol* 10: R605–R607, 2000.
- Carandini M, Ferster D.** A tonic hyperpolarization underlying contrast adaptation in cat visual cortex. *Science* 276: 949–952, 1997.
- Dragoi V, Rivadulla C, Sur M.** Foci of orientation plasticity in visual cortex. *Nature* 411: 80–86, 2001.
- Dragoi V, Sharma J, Sur M.** Adaptation-induced plasticity of orientation tuning in adult visual cortex. *Neuron* 28: 287–298, 2000.
- Fang F, Murray SO, Kersten D, He S.** Orientation-tuned fMRI adaptation in human visual cortex. *J Neurophysiol* 94: 4188–4195, 2005.
- Fried SI, Munch TA, Werblin FS.** Mechanisms and circuitry underlying directional selectivity in the retina. *Nature* 420: 411–414, 2002.
- Gardner JL, Sun P, Waggoner RA, Ueno K, Tanaka K, Cheng K.** Contrast adaptation and representation in human early visual cortex. *Neuron* 47: 607–620, 2005.
- Greenlee MW, Heitger F.** The functional role of contrast adaptation. *Vision Res* 28: 791–797, 1988.
- Haynes JD, Deichmann R, Rees G.** Eye-specific effects of binocular rivalry in the human lateral geniculate nucleus. *Nature* 438: 496–499, 2005.
- Jin DZ, Dragoi V, Sur M, Seung HS.** Tilt aftereffect and adaptation-induced changes in orientation tuning in visual cortex. *J Neurophysiol* 94: 4038–4050, 2005.
- Klein S, Stromeyer CF III, Ganz L.** The simultaneous spatial frequency shift: a dissociation between the detection and perception of gratings. *Vision Res* 14: 1421–1432, 1974.
- Larsson J, Landy MS, Heeger DJ.** Orientation-selective adaptation to first- and second-order patterns in human visual cortex. *J Neurophysiol* 95: 862–881, 2006.
- Maattanen LM, Koenderink JJ.** Contrast adaptation and contrast gain control. *Exp Brain Res* 87: 205–212, 1991.
- Maffei L, Fiorentini A, Bisti S.** Neural correlate of perceptual adaptation to gratings. *Science* 182: 1036–1038, 1973.
- Mante V, Frazor R, Bonin V, Geisler W, Carandini M.** Independence of luminance and contrast in natural scenes and in the early visual system. *Nat Neurosci* 8: 1690–1697, 2005.
- Movshon JA, Lennie P.** Pattern-selective adaptation in visual cortical neurones. *Nature* 278: 850–852, 1979.
- Muller JR, Metha AB, Krauskopf J, Lennie P.** Rapid adaptation in visual cortex to the structure of images. *Science* 285: 1405–1408, 1999.
- Ohzawa I, Sclar G, Freeman RD.** Contrast gain control in the cat visual cortex. *Nature* 298: 266–268, 1982.
- Ohzawa I, Sclar G, Freeman RD.** Contrast gain control in the cat's visual system. *J Neurophysiol* 54: 651–667, 1985.
- Reid RC, Victor JD, Shapley RM.** The use of m-sequences in the analysis of visual neurons: linear receptive field properties. *Vis Neurosci* 14: 1015–1027, 1997.
- Ross J, Speed HD.** Perceived contrast following adaptation to gratings of different orientations. *Vision Res* 36: 1811–1818, 1996.
- Sanchez-Vives MV, Nowak LG, McCormick DA.** Cellular mechanisms of long-lasting adaptation in visual cortical neurons in vitro. *J Neurosci* 20: 4286–4299, 2000a.
- Sanchez-Vives MV, Nowak LG, McCormick DA.** Membrane mechanisms underlying contrast adaptation in cat area 17 in vivo. *J Neurosci* 20: 4267–4285, 2000b.
- Saul AB, Cynader MS.** Adaptation in single units in visual cortex: the tuning of aftereffects in the spatial domain. *Vis Neurosci* 2: 593–607, 1989.
- Sclar G, Ohzawa I, Freeman RD.** Contrast gain control in the kitten's visual system. *J Neurophysiol* 54: 668–675, 1985.
- Shou T, Li X, Zhou Y, Hu B.** Adaptation of visually evoked responses of relay cells in the dorsal lateral geniculate nucleus of the cat following prolonged exposure to drifting gratings. *Vis Neurosci* 13: 605–613, 1996.

- Smirnakis SM, Berry MJ, Warland DK, Bialek W, Meister M.** Adaptation of retinal processing to image contrast and spatial scale. *Nature* 386: 69–73, 1997.
- Snowden RJ, Hammett ST.** Subtractive and divisive adaptation in the human visual system. *Nature* 355: 248–250, 1992.
- Snowden RJ, Hammett ST.** Spatial frequency adaptation: threshold elevation and perceived contrast. *Vision Res* 36: 1797–1809, 1996.
- Solomon SG, Peirce JW, Dhruv NT, Lennie P.** Profound contrast adaptation early in the visual pathway. *Neuron* 42: 155–162, 2004.
- Xue JT, Ramoa AS, Carney T, Freeman RD.** Binocular interaction in the dorsal lateral geniculate nucleus of the cat. *Exp Brain Res* 68: 305–310, 1987.